



Physics-based control-oriented modeling of the current density profile evolution in NSTX-Upgrade



Zeki O. Ilhan^{a,*}, Justin E. Barton^a, Eugenio Schuster^a, David A. Gates^b, Stefan P. Gerhardt^b, Jonathan E. Menard^b

^a Department of Mechanical Engineering and Mechanics, Lehigh University, Bethlehem, PA 18015, USA

^b Princeton Plasma Physics Laboratory, Princeton, NJ 08540, USA

HIGHLIGHTS

- A physics-based, control-oriented model describing the temporal evolution of the current density profile in tokamaks is obtained by combining the magnetic diffusion equation with empirical correlations for the electron density, electron temperature, and non-inductive current drives.
- The resulting first-principles-driven control-oriented model is tailored to the National Spherical Torus eXperiment-Upgrade (NSTX-U) based on the predictions of the TRANSP simulation code.
- The model's prediction capabilities are illustrated by comparing simulated data to TRANSP predictions for a reference run.
- Objectives and possible challenges associated with the use of the proposed model for the design of both feedforward and feedback controllers are discussed.

ARTICLE INFO

Article history:

Received 3 October 2016

Received in revised form 9 March 2017

Accepted 7 April 2017

Available online 11 May 2017

Keywords:

Plasma engineering
Tokamak plasma control
Current profile control
Model-based control

ABSTRACT

Active control of the toroidal current density profile is among those plasma control milestones that the National Spherical Torus eXperiment-Upgrade (NSTX-U) program must achieve to realize its next-step operational goals. Motivated by the coupled, nonlinear, multivariable, distributed-parameter plasma dynamics, the first step towards control design is the development of a physics-based, control-oriented model for the current profile evolution in response to non-inductive current drives and heating systems. The evolution of the toroidal current density profile is closely related to the evolution of the poloidal magnetic flux profile, whose dynamics is modeled by a nonlinear partial differential equation (PDE) referred to as the magnetic-flux diffusion equation (MDE). The proposed control-oriented model predicts the spatial-temporal evolution of the current density profile by combining the nonlinear MDE with physics-based correlations obtained at NSTX-U for the electron density, electron temperature, and non-inductive current drives (neutral beams). The resulting first-principles-driven, control-oriented model is tailored for NSTX-U based on predictions by the time-dependent transport code TRANSP. Main objectives and possible challenges associated with the use of the developed model for the design of both feedforward and feedback controllers are also discussed.

© 2017 Elsevier B.V. All rights reserved.

1. Introduction

The National Spherical Torus eXperiment-Upgrade (NSTX-U), located at the Princeton Plasma Physics Laboratory (PPPL) in the USA, is one of the major spherical torus (ST) experimental facilities in the world. NSTX-U is a substantial upgrade of the former NSTX device, with significantly higher toroidal field and

solenoid capabilities, and three additional neutral beam sources with significantly larger current-drive efficiency [1].

Active control of the toroidal current density profile is among those plasma control milestones that the NSTX-U program must achieve to realize its next-step operational goals characterized by a high-performance, MHD-stable, plasma operation with neutral beam heating and longer pulse durations [1]. As a first step towards control design, the goal of this work is to convert the physics-based model of the poloidal magnetic flux profile evolution [2], which is related to the toroidal current density profile evolution in the spherical torus, into a form suitable for control design. This is

* Corresponding author.

E-mail address: ilhan@alum.lehigh.edu (Z.O. Ilhan).

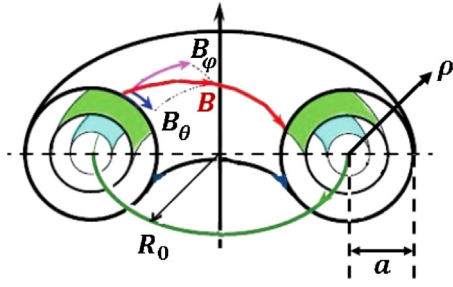


Fig. 1. Magnetic flux surfaces in a tokamak [8]. The helical magnetic field (\vec{B}) in a tokamak plasma is composed of toroidal (\vec{B}_ϕ) and poloidal (\vec{B}_θ) fields. The poloidal magnetic flux is defined as $\Psi = \int \vec{B}_\theta \cdot \vec{n} dA_z$, where A_z denotes the area of a disc of radius R , and \vec{n} is the unit vector perpendicular to the disk. Also shown are the geometric major radius, R_0 , and the minor radius, a .

achieved by combining the magnetic flux diffusion equation with physics-based control-oriented models for the electron density and temperature profiles, the plasma resistivity, and the non-inductive current-drives, thereby obtaining a first-principles-driven (FPD) model. The resulting control-oriented FPD model needs only to capture the dominant physics that describe how the control actuators affect the poloidal magnetic flux evolution. Numerical simulations of the proposed control-oriented model show qualitative agreement with the physics-based transport code TRANSP [3].

The proposed FPD model can be used to design both feedforward and feedback controllers to regulate the current-density profile dynamics in NSTX-U. The goal of the feedforward control design stage is to produce actuator trajectories that can steer the plasma to a desired operating state. The main challenge arising during this stage is the trade-off between the complexity of the plasma response model and the computational time required to solve the feedforward control optimization. However, the uncertainty in the FPD model (and hence in the feedforward actuator trajectories) arising from limiting its complexity can be compensated by complementing the feedforward control solution with feedback control. The proposed FPD model has already been employed for the design of both optimal [4] and predictive [5] feedback control strategies to add robustness to the overall current profile control scheme in NSTX-U.

2. Current density profile evolution model

Any arbitrary quantity that is constant on each magnetic flux surface within the tokamak plasma can be used to index the flux surfaces, which are graphically depicted in Fig. 1. In this work, we choose the mean effective minor radius, ρ , of the flux surface, i.e., $\pi B_{\phi,0} \rho^2 = \Phi$, as the indexing variable, where Φ is the toroidal magnetic flux and $B_{\phi,0}$ is the vacuum toroidal magnetic field at the geometric major radius R_0 of the tokamak. The normalized effective minor radius is defined as $\hat{\rho} = \rho/\rho_b$, where ρ_b is the mean effective minor radius of the last closed flux surface. The safety factor profile (q) and the toroidal current density profile (j_ϕ) are related through

$$q(\hat{\rho}, t) = \frac{\hat{\rho}^2 B_\phi}{R_0 \mu_0} \frac{1}{\int_0^{\hat{\rho}} j_\phi(\hat{\rho}', t) \hat{\rho}' d\hat{\rho}'}, \quad (1)$$

where μ_0 is the permeability of the free space [6]. Therefore, the toroidal current density can be specified indirectly by the safety factor q , which is also defined as $q(\hat{\rho}, t) = -d\Phi/d\Psi$ [6], where Ψ

is the poloidal magnetic flux. Using $\Phi = \pi B_{\phi,0} \rho^2$ and $\hat{\rho} = \rho/\rho_b$, the q -profile can be expressed as

$$q(\hat{\rho}, t) = -\frac{d\Phi}{d\Psi} = -\frac{d\Phi}{2\pi d\psi} = -\frac{\frac{\partial\Phi}{\partial\rho} \frac{\partial\rho}{\partial\hat{\rho}}}{2\pi \frac{\partial\psi}{\partial\hat{\rho}}} = -\frac{B_{\phi,0} \rho_b^2 \hat{\rho}}{\partial\psi/\partial\hat{\rho}}, \quad (2)$$

where $\psi(\hat{\rho}, t)$ is the poloidal stream function, which is closely related to the poloidal flux Ψ ($\Psi = 2\pi\psi$).

Combining (1) and (2), it can be shown that the control of the current density profile $j_\phi(\hat{\rho}, t)$ is equivalent to the control of the q -profile, which in turn is equivalent to the control of the poloidal flux gradient profile $\partial\psi/\partial\hat{\rho}$. The evolution of the poloidal magnetic flux ψ is given by the magnetic diffusion equation (MDE) [7]

$$\frac{\partial\psi}{\partial t} = \frac{\eta(T_e)}{\mu_0 \rho_b^2 \hat{F}^2} \frac{1}{\hat{\rho}} \frac{\partial}{\partial\hat{\rho}} \left(\hat{\rho} D_\psi \frac{\partial\psi}{\partial\hat{\rho}} \right) + R_0 \hat{H} \eta(T_e) \frac{\langle \vec{j}_{ni} \cdot \vec{B} \rangle}{B_{\phi,0}}, \quad (3)$$

with boundary conditions:

$$\frac{\partial\psi}{\partial\hat{\rho}} \Big|_{\hat{\rho}=0} = 0, \quad \frac{\partial\psi}{\partial\hat{\rho}} \Big|_{\hat{\rho}=1} = -k_{I_p} I_p(t), \quad (4)$$

where η is the plasma resistivity, T_e is the electron temperature, μ_0 is the vacuum permeability, \vec{j}_{ni} is any source of noninductive current density, \vec{B} is the magnetic field, $\langle \cdot \rangle$ denotes a flux-surface average, $D_\psi(\hat{\rho}) = \hat{F}(\hat{\rho}) \hat{G}(\hat{\rho}) \hat{H}(\hat{\rho})$, where

$$\hat{F} = \frac{R_0 B_{\phi,0}}{R B_\phi(R, Z)}, \quad \hat{G} = \left\langle \frac{R_0^2}{R^2} |\nabla\rho|^2 \right\rangle, \quad \hat{H} = \frac{\hat{F}}{(R_0^2/R^2)},$$

are geometric factors pertaining to the magnetic configuration of a particular plasma equilibrium, $I_p(t)$ is the total plasma current, and $k_{I_p} = \mu_0 R_0 / [2\pi \hat{G}(1) \hat{H}(1)]$.

3. Control-oriented modeling of plasma parameters

In this section, empirical models are developed based on both physical observations and simulations for the electron density and temperature profiles, the noninductive current sources, and the plasma resistivity for a general NSTX-U operating scenario in order to close the magnetic diffusion equation model (3) and to obtain a control-oriented FPD model of the poloidal flux profile evolution. It is important to emphasize that the models developed in this section are not designed for physical understanding, rather they are meant to capture the dominant physics that describe how the control actuators affect the plasma properties, and hence the current density profile evolution.

3.1. Electron density modeling

The electron density profile $n_e(\hat{\rho}, t)$ is modeled as

$$n_e(\hat{\rho}, t) = n_e^{prof}(\hat{\rho}) u_n(t), \quad (5)$$

where $n_e^{prof}(\hat{\rho})$ is a reference profile and $u_n(t)$ regulates the time evolution of the electron density. Note that n_e^{prof} is obtained by evaluating the experimental or simulated n_e profile at a reference time $t_{r_{n_e}}$, i.e., $n_e^{prof}(\hat{\rho}) = n_e(\hat{\rho}, t_{r_{n_e}})$, and the electron density regulation term $u_n(t)$ is obtained from $u_n(t) = \int_0^1 n_e(\hat{\rho}, t) \frac{\partial V}{\partial\hat{\rho}} d\hat{\rho} / \int_0^1 n_e^{prof}(\hat{\rho}) \frac{\partial V}{\partial\hat{\rho}} d\hat{\rho}$, where V denotes the volume enclosed by a magnetic surface. This model assumes the control action employed to regulate the electron density weakly affects the radial distribution of the electrons.

3.2. Electron temperature modeling

In the formulation of the electron temperature model, we assume a tight coupling between the plasma electron and ion

species, i.e., $T_e(\hat{\rho}, t) \approx T_i(\hat{\rho}, t)$ and $n_e(\hat{\rho}, t) \approx n_i(\hat{\rho}, t)$, where $T_i(\hat{\rho}, t)$ and $n_i(\hat{\rho}, t)$ are the ion temperature and density profiles, respectively. This assumption could be eliminated if necessary at the expense of a slightly more complex model. The electron temperature profile is modeled as

$$T_e(\hat{\rho}, t) = k_{T_e}(\hat{\rho}) \frac{T_e^{prof}(\hat{\rho})}{n_e(\hat{\rho}, t)} I_p(t) \sqrt{P_{tot}(t)}, \quad (6)$$

where $k_{T_e}(\hat{\rho})$ is a constant, $T_e^{prof}(\hat{\rho})$ is a reference profile, and $P_{tot}(t)$ is the total power injected into the plasma. Note that $T_e^{prof}(\hat{\rho})$ is evaluated at a reference time $t_{r_{T_e}}$, i.e., $T_e^{prof}(\hat{\rho}) = T_e(\hat{\rho}, t_{r_{T_e}})$. The constant $k_{T_e}(\hat{\rho})$ is expressed as $k_{T_e}(\hat{\rho}) = n_e(\hat{\rho}, t_{r_{T_e}}) / [I_p(t_{r_{T_e}}) P_{tot}(t_{r_{T_e}})^{1/2}]$.

The total power injected into the plasma, $P_{tot}(t)$ is expressed as $P_{tot}(t) = P_{ohm}(t) + P_{aux}(t) - P_{rad}(t)$, where $P_{ohm}(t)$ is the ohmic power, $P_{aux}(t)$ is the total auxiliary heating/current-drive (H&CD) power and $P_{rad}(t)$ is the radiated power. The ohmic power is modeled as $P_{ohm}(t) \approx 2\pi R_0 I_p(t)^2 / \int_0^1 \frac{1}{\eta(\hat{\rho}, t)} \frac{dS}{d\hat{\rho}} d\hat{\rho}$, where S denotes a magnetic surface within the plasma. The total auxiliary H&CD power is expressed as $P_{aux}(t) = \sum_{i=1}^{n_{nbi}} P_{nbi}(t)$, where $P_{nbi}(t)$ is the individual neutral beam injector powers, and n_{nbi} is the total number of neutral beam launchers. The radiative power density losses are modeled in [6] as $Q_{rad} = k_{brem} Z_{eff} n_e(\hat{\rho}, t)^2 \sqrt{T_e(\hat{\rho}, t)}$, where $k_{brem} = 5.5 \times 10^{-37} \text{ W m}^3 / \sqrt{\text{keV}}$ is the Bremsstrahlung radiation coefficient and Z_{eff} is the effective atomic number of the ions in the plasma, which is assumed to be a constant in space and time. The radiated power is then expressed as $P_{rad}(t) = \int_0^1 Q_{rad}(\hat{\rho}, t) \frac{dV}{d\hat{\rho}} d\hat{\rho}$. Note that, if necessary, sources of radiation different from Bremsstrahlung radiation could also be included in the model.

3.3. Plasma resistivity modeling

The resistivity η scales with the electron temperature as

$$\eta(\hat{\rho}, t) = \frac{k_{sp}(\hat{\rho}) Z_{eff}}{T_e(\hat{\rho}, t)^{3/2}}, \quad (7)$$

where $k_{sp}(\hat{\rho}) = [\eta(\hat{\rho}, t_{r_\eta}) T_e(\hat{\rho}, t_{r_\eta})^{3/2}] / Z_{eff}$ is a constant that is evaluated at a reference time t_{r_η} .

3.4. Noninductive current-drive modeling

The total noninductive current-drive in NSTX-U is produced by the auxiliary neutral beam launchers and the bootstrap current, and is expressed as

$$\frac{(\bar{j}_{ni} \cdot \bar{B})}{B_{\phi,0}} = \sum_{i=1}^{n_{nbi}} \frac{(\bar{j}_i \cdot \bar{B})}{B_{\phi,0}} + \frac{(\bar{j}_{bs} \cdot \bar{B})}{B_{\phi,0}}, \quad (8)$$

where \bar{j}_i is the noninductive current density generated by the individual neutral beam injectors, and \bar{j}_{bs} is the noninductive current density generated by the bootstrap effect [9].

3.4.1. Neutral beam injection current-drive

We model each auxiliary noninductive-current source as the time-varying source power multiplied by a constant deposition profile in space and the efficiency of the source. Therefore, the noninductive toroidal current density provided by each individual neutral beam injector is modeled as

$$\frac{(\bar{j}_i \cdot \bar{B})}{B_{\phi,0}}(\hat{\rho}, t) = k_{nbi}(\hat{\rho}) j_{nbi}^{dep}(\hat{\rho}) \frac{\sqrt{T_e(\hat{\rho}, t)}}{n_e(\hat{\rho}, t)} P_{nbi}(t), \quad (9)$$

where $i = [1, 2, \dots, n_{nbi}]$, $k_{nbi}(\hat{\rho})$ is a normalizing profile, $j_{nbi}^{dep}(\hat{\rho})$ is a reference profile for each current-drive source, and the term $\sqrt{T_e}/n_e$ represents the current-drive efficiency. Note that $j_{nbi}^{dep}(\hat{\rho})$ is evaluated at a reference time $t_{r_{nbi}}$, i.e., $j_{nbi}^{dep}(\hat{\rho}) = [(\bar{j}_i \cdot \bar{B})/B_{\phi,0}](\hat{\rho}, t_{r_{nbi}})$. The constants $k_{nbi}(\hat{\rho})$ are expressed as $k_{nbi}(\hat{\rho}) = n_e(\hat{\rho}, t_{r_{nbi}}) / [\sqrt{T_e(\hat{\rho}, t_{r_{nbi}})} P_{nbi}(t_{r_{nbi}})]$.

3.4.2. Bootstrap current-drive

The bootstrap current is directly related to the inhomogeneity of the magnetic field strength $B \propto 1/R$, and is associated with trapped particles [9]. From [10], the bootstrap current model is

$$\frac{(\bar{j}_{bs} \cdot \bar{B})}{B_{\phi,0}}(\hat{\rho}, t) = \frac{R_0}{\bar{F}} \left(\frac{\partial \psi}{\partial \hat{\rho}} \right)^{-1} \times \left[2\mathcal{L}_{31} T_e \frac{\partial n_e}{\partial \hat{\rho}} + \{2\mathcal{L}_{31} + \mathcal{L}_{32} + \alpha \mathcal{L}_{34}\} n_e \frac{\partial T_e}{\partial \hat{\rho}} \right], \quad (10)$$

where \mathcal{L}_{31} , \mathcal{L}_{32} , \mathcal{L}_{34} , and α are functions of $\hat{\rho}$.

4. FPD model of poloidal magnetic flux profile evolution

By substituting the simplified physics-based models for the electron density (5), electron temperature (6), plasma resistivity (7), and noninductive current-drives (8)–(10) into the MDE (3), space and time functions can be separated. As a result, the MDE takes the control-oriented form

$$\frac{\partial \psi}{\partial t} = f_\eta u_\eta \frac{1}{\hat{\rho}} \frac{\partial}{\partial \hat{\rho}} \left(\hat{\rho} D_\psi \frac{\partial \psi}{\partial \hat{\rho}} \right) + \sum_{i=1}^{n_{nbi}} f_i u_i + f_{bs} u_{bs} \left(\frac{\partial \psi}{\partial \hat{\rho}} \right)^{-1}, \quad (11)$$

with boundary conditions $\frac{\partial \psi}{\partial \hat{\rho}}|_{\hat{\rho}=0} = 0$ and $\frac{\partial \psi}{\partial \hat{\rho}}|_{\hat{\rho}=1} = -k_{ip} u_{ip}$, where the spatial functions f_η , f_i , and f_{bs} can be expressed in terms of the various model reference profiles and coefficients. The diffusivity (u_η), interior (u_i , u_{bs}) and boundary (u_{ip}) control terms are nonlinear combinations of the physical actuators defined as $u_\eta(t) = u_n(t)^{3/2} I_p(t)^{-3/2} P_{tot}(t)^{-3/4}$, $u_i(t) = P_{nbi}(t) I_p(t)^{-1} P_{tot}(t)^{-1/2}$, $u_{bs}(t) = u_n(t)^{3/2} I_p(t)^{-1/2} P_{tot}(t)^{-1/4}$, and $u_{ip}(t) = I_p(t)$. Simulation and/or experimental data can now be utilized to identify the model reference profiles and constants in the simplified physics-based models (5)–(10) to tailor the FPD model (11) to a scenario of interest in NSTX-U.

5. FPD model tailored to NSTX-U

Although NSTX-Upgrade was completed in 2015, plasma scenarios relevant to this work have not been achieved yet. Therefore, predictions by the physics-oriented transport code TRANSP [3] have been used to tailor the proposed FPD model to the geometry and actuators of NSTX-U.

There are 6 neutral beam launchers in NSTX-U, hence, $n_{nbi} = 6$ in (8). Note that for simplicity, all model reference profiles and coefficients, $n_e^{prof}(\hat{\rho})$, $T_e^{prof}(\hat{\rho})$, $j_{nbi}^{dep}(\hat{\rho})$, $k_{T_e}(\hat{\rho})$, $k_{sp}(\hat{\rho})$, and $k_{nbi}(\hat{\rho})$, are evaluated at the same reference time, $t_r = 4$ s. Therefore, $t_r = t_{r_{n_e}} = t_{r_{T_e}} = t_{r_\eta} = t_{r_{nbi}} = 4$ s. The physical inputs used during the simulations carried out based on both the FPD model and TRANSP are shown in Fig. 2(a). The parameters related to the magnetic configuration of the plasma equilibrium and the reference profiles and coefficients for the various models are shown in Fig. 2(b)–(f). Finally, Fig. 3 compares FPD-model-predicted and TRANSP-predicted $n_e(\hat{\rho})$, $T_e(\hat{\rho})$, $\eta(\hat{\rho})$, and $q(\hat{\rho})$ profiles at various instants.

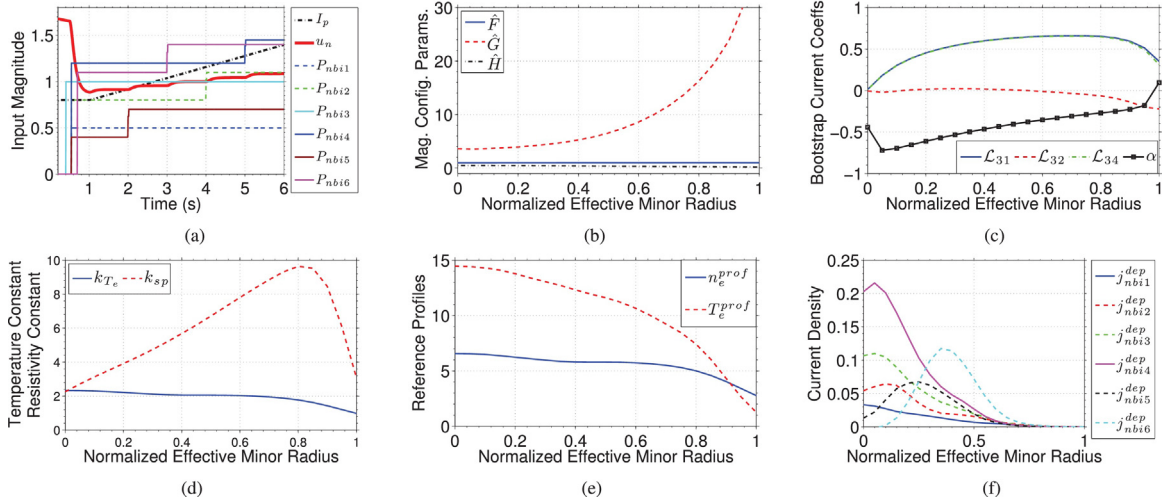


Fig. 2. (a) Physical inputs applied during the simulations based on both the FPD model and TRANSP (current in MA, power in MW, and u_n is dimensionless). (b)–(f) Model parameters tailored to NSTX-U: (b) Magnetic equilibrium configuration parameters $\hat{F}(\hat{\rho})$, $\hat{G}(\hat{\rho})$, and $\hat{H}(\hat{\rho})$, (c) bootstrap current coefficients $\mathcal{L}_{31}(\hat{\rho})$, $\mathcal{L}_{32}(\hat{\rho})$, $\mathcal{L}_{34}(\hat{\rho})$ and $\alpha(\hat{\rho})$, (d) electron temperature coefficient k_{Te} ($10^{10} \text{ m}^{-3} \text{ A}^{-1} \text{ W}^{-1/2}$) and plasma resistivity coefficient k_{sp} ($10^{-8} \Omega \text{ m keV}^{3/2}$), (e) reference electron density $n_e^{prof}(\hat{\rho})$ and electron temperature $T_e^{prof}(\hat{\rho})$ profiles, and (f) reference neutral beam current deposition profiles for individual beams $j_{nbi_i}^{dep}(\hat{\rho})$.

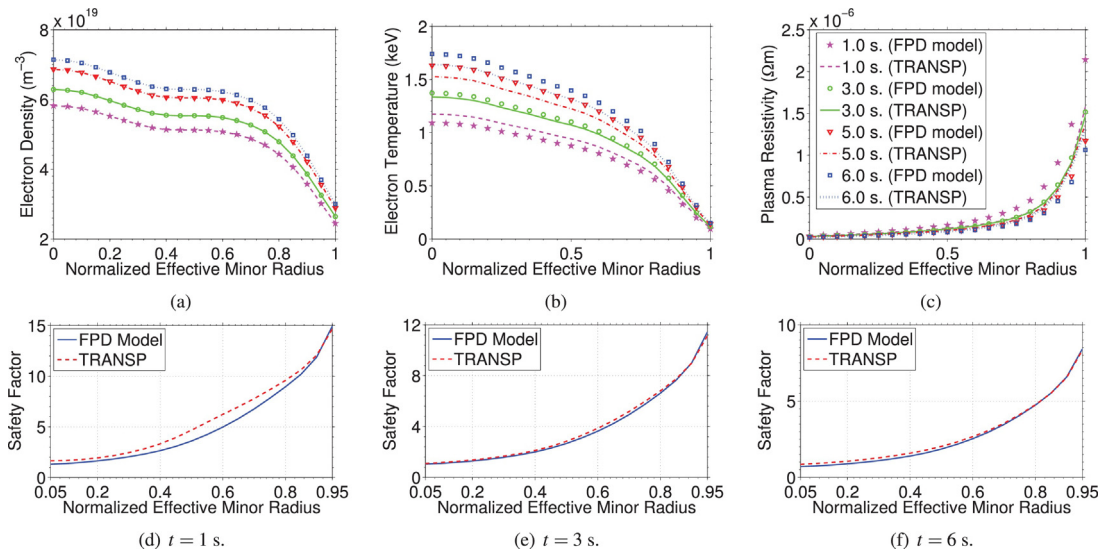


Fig. 3. Comparison of the TRANSP predicted and FPD model predicted (a) electron density $n_e(\hat{\rho})$, (b) electron temperature $T_e(\hat{\rho})$, (c) plasma resistivity $\eta(\hat{\rho})$, and (d)–(f) comparison of the safety factor $q(\hat{\rho})$ profiles at various instants. Figures (a) and (b) share the same legend as that provided for Figure (c).

As can be seen from Fig. 3(a), the FPD model and TRANSP show perfect agreement in predicting the n_e profile because they share the same model. Although Fig. 3(b) and (c) show that the FPD model captures the main dynamics affecting the evolution of the T_e and η profiles for the purposes of control design, the observed mismatches could be improved at the expense of adding more complexity to the present model for T_e . Finally, as can be seen from Fig. 3(d)–(f), the TRANSP-predicted and FPD-model-predicted q profiles seem to show the level of agreement that is needed for control design purposes.

6. Conclusions and future work

In this work, the nonlinear magnetic-diffusion PDE has been coupled with empirical models for the electron density, electron temperature, plasma resistivity and noninductive current drive

(neutral beams and bootstrap) to produce a first-principles-driven (FPD) control-oriented model of the current profile response in NSTX-U. Simulations based on the FPD model carried out in just a few seconds provide good agreement with TRANSP predictions that take several hours, indicating that the accuracy level provided by the FPD control-oriented model is adequate for control design purposes. Although it is always possible to improve the prediction accuracy by adding more complexity to the T_e and η models, a more important next-step goal is to refine the FPD model using actual experimental data once NSTX-U begins producing meaningful plasmas. This would improve prediction accuracy for more reliable design and testing of various control algorithms.

Acknowledgement

Work supported by the US DoE (DE-AC02-09CH11466).

References

- [1] S.P. Gerhardt, et al., Exploration of the equilibrium operating space for NSTX-Upgrade, *Nuclear Fusion* 52 (8) (2012) 083020.
- [2] F. Hinton, R. Hazeltine, Theory of plasma transport in toroidal confinement systems, *Rev. Mod. Phys.* 48 (1976) 239–308.
- [3] TRANSP Homepage, 2015, <http://w3.pppl.gov/transp/>.
- [4] Z. Ilhan, W. Wehner, et al., First-principles-driven model-based optimal control of the current profile in NSTX-U, in: *IEEE Conference on Control Applications (CCA)*, 2015, pp. 1303–1308.
- [5] Z. Ilhan, W. Wehner, E. Schuster, Model predictive control with integral action for the rotational transform profile tracking in NSTX-U, in: *IEEE Conference on Control Applications (CCA)*, 2016, pp. 623–628.
- [6] J. Wesson, *Tokamaks*, Clarendon Press, Oxford, UK, 1984.
- [7] Y. Ou, et al., Towards model-based current profile control at DIII-D, *Fusion Eng. Des.* 82 (2007) 1153–1160.
- [8] B.L. Tan, G.L. Huang, Neoclassical bootstrap current in solar plasma loops, *Astron. Astrophys.* 453 (1) (2006) 321–327.
- [9] A.G. Peeters, The bootstrap current and its consequences, *Plasma Phys. Control. Fusion* 42 (2000) B231–B242.
- [10] O. Sauter, et al., Neoclassical conductivity and bootstrap current formulas for general axisymmetric equilibria and arbitrary collisionality regime, *Phys. Plasmas* 6 (7) (1999) 2834.